



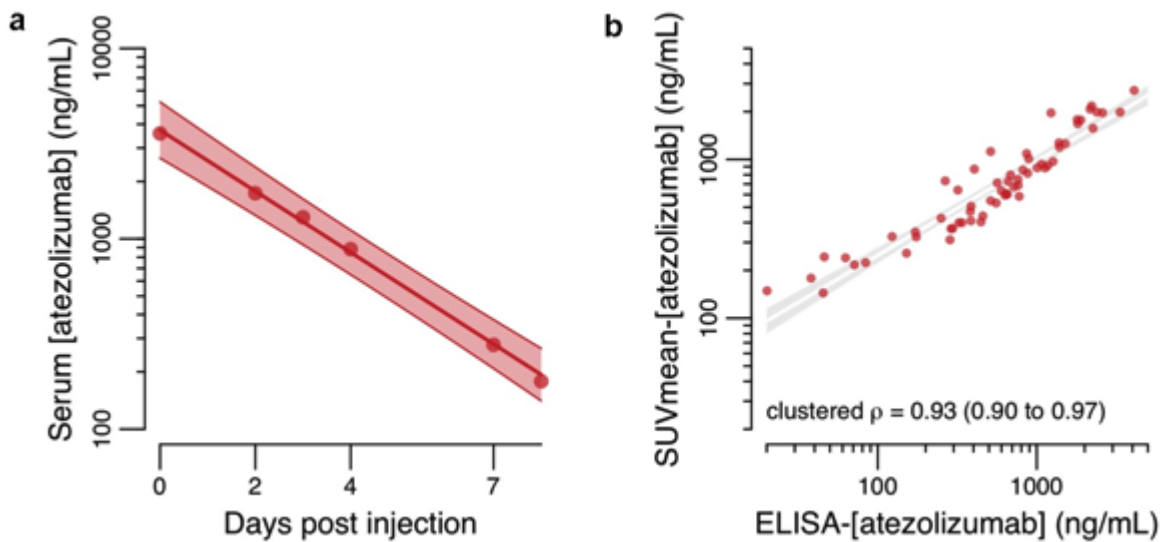
In the format provided by the authors and unedited.

# **$^{89}\text{Zr}$ -atezolizumab imaging as a non-invasive approach to assess clinical response to PD-L1 blockade in cancer**

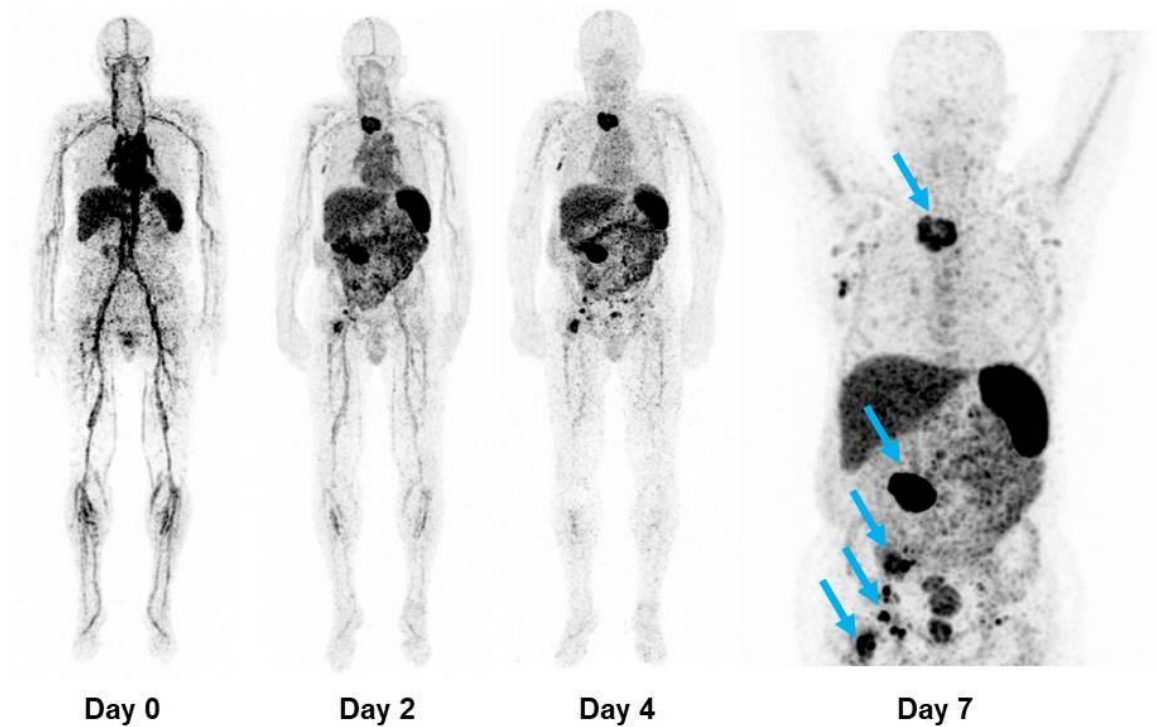
**Frederike Bensch<sup>1</sup>, Elly L. van der Veen<sup>1</sup>, Marjolijn N. Lub-de Hooge<sup>2,3</sup>, Annelies Jorritsma-Smit<sup>2</sup>, Ronald Boellaard<sup>3</sup>, Iris C. Kok<sup>1</sup>, Sjoukje F. Oosting<sup>1</sup>, Carolina P. Schröder<sup>1</sup>, T. Jeroen N. Hiltermann<sup>4</sup>, Anthonie J. van der Wekken<sup>4</sup>, Harry J. M. Groen<sup>4</sup>, Thomas C. Kwee<sup>3</sup>, Sjoerd G. Elias<sup>5</sup>, Jourik A. Gietema<sup>1</sup>, Sandra Sanabria Bohorquez<sup>6</sup>, Alex de Crespigny<sup>6</sup>, Simon-Peter Williams<sup>6</sup>, Christoph Mancao<sup>7</sup>, Adrienne H. Brouwers<sup>3</sup>, Bernard M. Fine<sup>6</sup> <sup>6</sup> and Elisabeth G. E. de Vries<sup>1\*</sup> <sup>1\*</sup>**

---

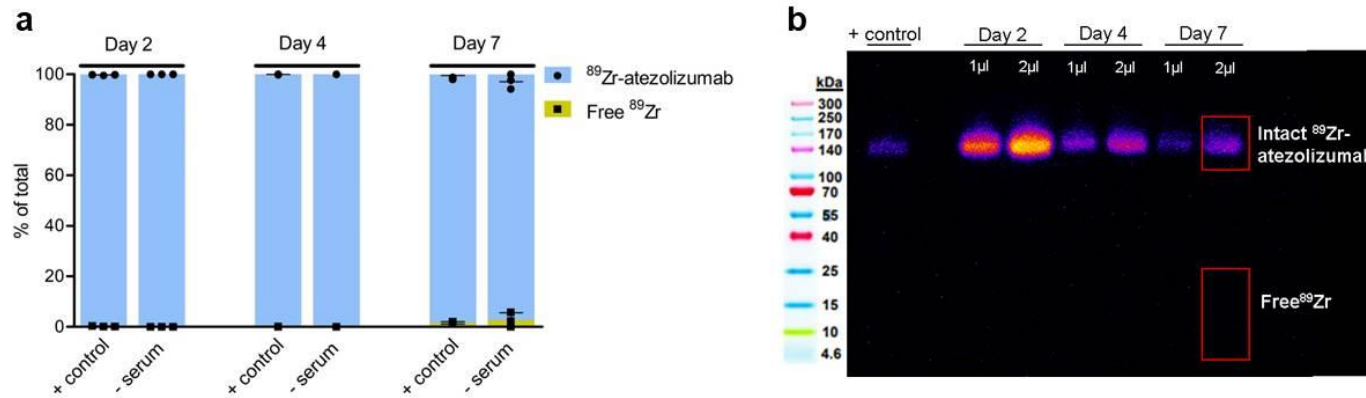
<sup>1</sup>Department of Medical Oncology, University Medical Center Groningen, University of Groningen, Groningen, the Netherlands. <sup>2</sup>Clinical Pharmacy and Pharmacology, University Medical Center Groningen, University of Groningen, Groningen, the Netherlands. <sup>3</sup>Medical Imaging Center, University Medical Center Groningen, University of Groningen, Groningen, the Netherlands. <sup>4</sup>Pulmonary Oncology, University Medical Center Groningen, University of Groningen, Groningen, the Netherlands. <sup>5</sup>Department of Epidemiology, Julius Center for Health Sciences and Primary Care, University Medical Center Utrecht, Utrecht University, Utrecht, the Netherlands. <sup>6</sup>Genentech, San Francisco, CA, USA. <sup>7</sup>Genentech, Basel, Switzerland. \*e-mail: [e.g.e.de.vries@umcg.nl](mailto:e.g.e.de.vries@umcg.nl)



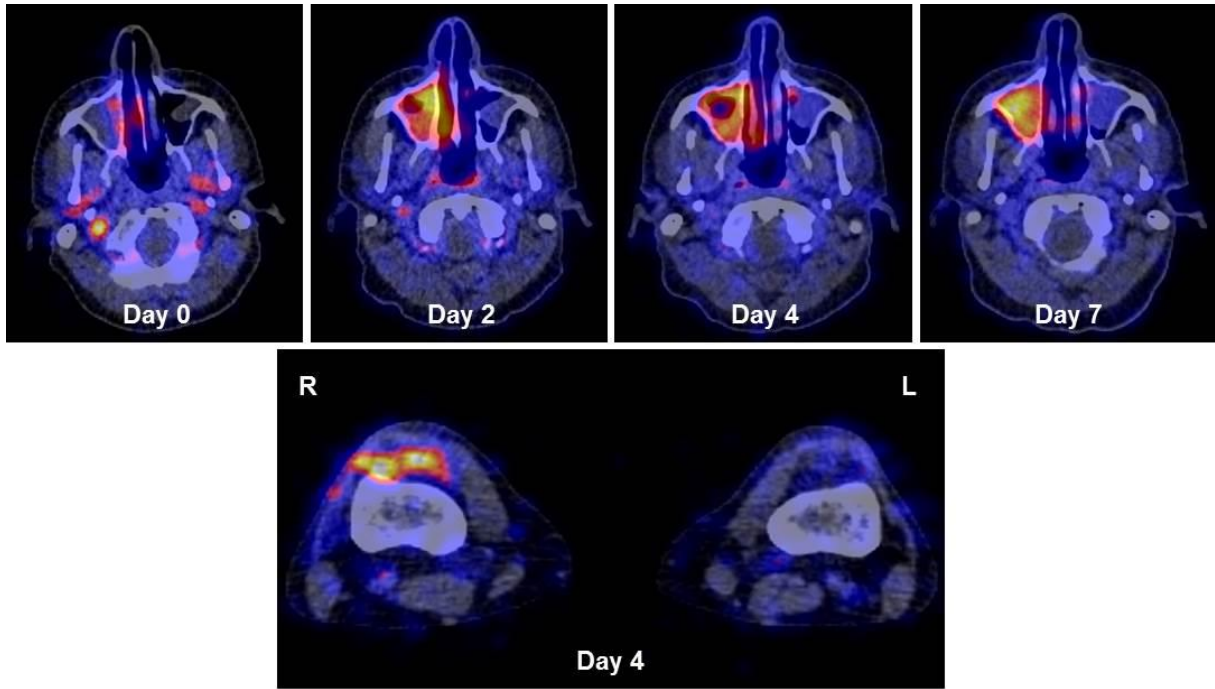
1  
2 **Supplementary Figure 1** Atezolizumab pharmacokinetics. (a) Atezolizumab serum  
3 concentration (ng/mL) over time plotted as geometric means per time point, including fitted  
4 regression line with 95%CI based on a linear mixed effect model with 62 measurements from  
5 22 patients. (b) Scatter plot of PET derived atezolizumab concentration and ELISA derived  
6 atezolizumab serum concentration (both ng/mL) and regression line with 95%CI based on a  
7 linear mixed effect model with 62 measurements from 22 patients;  $\rho$ : Pearson's correlation  
8 coefficient extended to clustered data with 95%CI.



9  
 10 **Supplementary Figure 2** <sup>89</sup>Zr-atezolizumab biodistribution. Representative PET images  
 11 (maximum intensity projections) of a patient one hour post tracer injection, and at days 2, 4  
 12 and 7. Multiple bone lesions, malignant inguinal and mediastinal lymphadenopathy and a big  
 13 abdominal wall metastasis are indicated with blue arrows on the last PET scan 7 days  
 14 postinjection (PET scans were performed once per patient and time point).

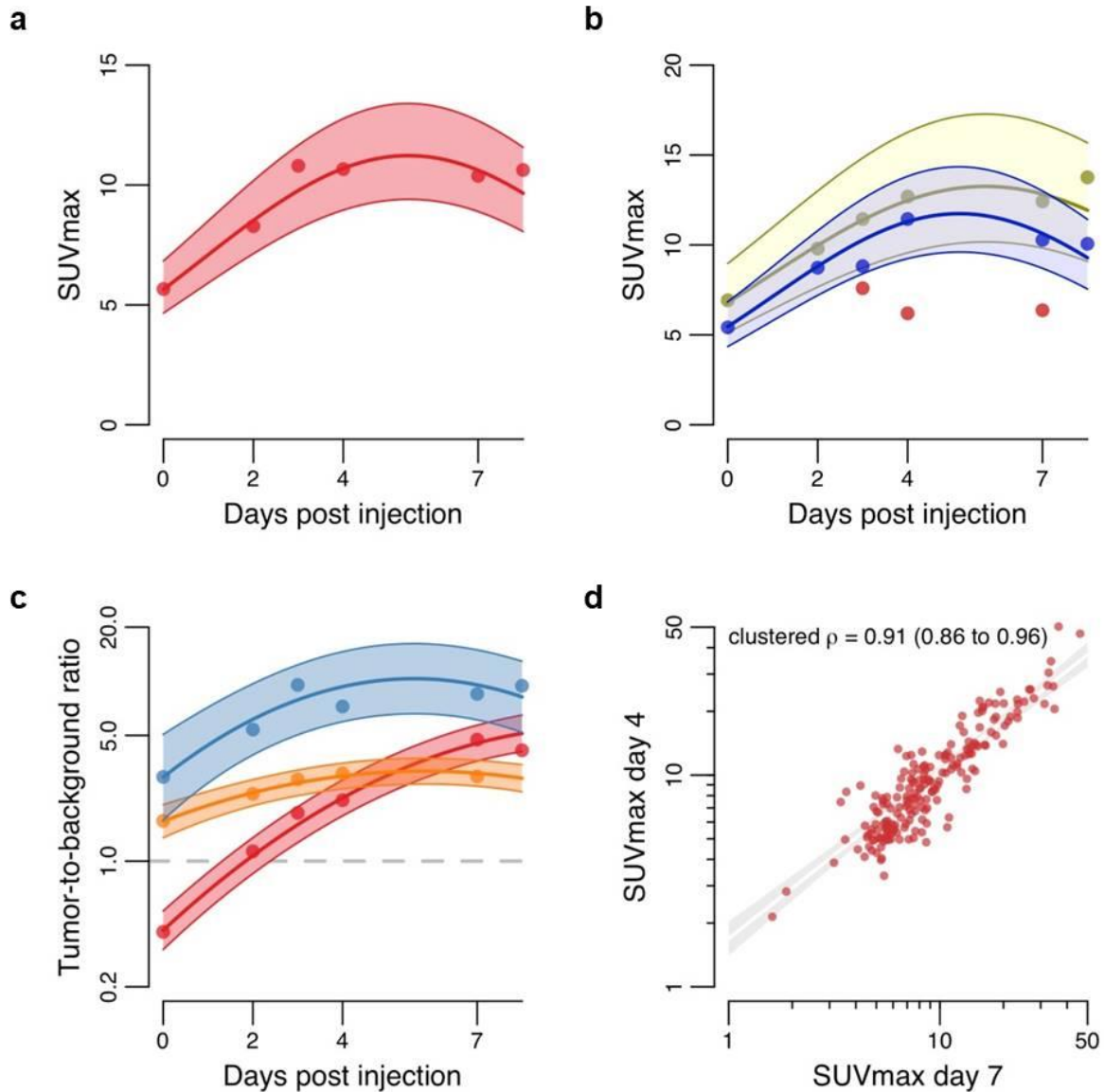


15 **Supplementary Figure 3** Intactness of  $^{89}\text{Zr}$ -atezolizumab over time. (a) Stability of  $^{89}\text{Zr}$ -atezolizumab determined by SDS-PAGE in patients' blood samples drawn 2, 4 and 7 days postinjection ( $n = 3$  biologically independent samples). Positive control (+ control) is  $^{89}\text{Zr}$ -atezolizumab stored at 2-8°C. Mean with error bars indicating standard deviation. (b) Representative example of an SDS-PAGE (SDS-PAGE was performed once per sample).



19

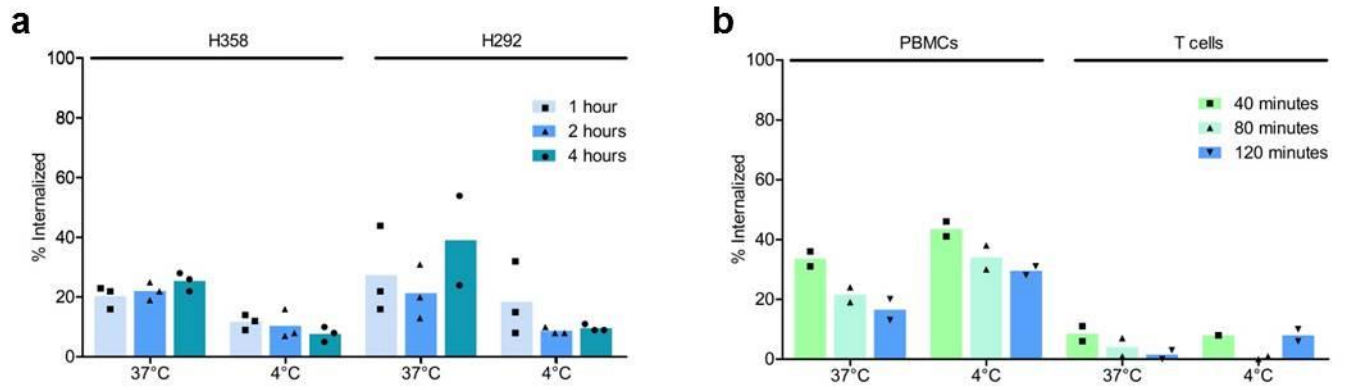
20 **Supplementary Figure 4**  $^{89}\text{Zr}$ -atezolizumab uptake in sites of inflammation. Upper panel  
21 shows transversal PET/LD CT images of a patient with chronic sinusitis with increasing tracer  
22 uptake over time. Lower panel shows increased tracer uptake in a patient with bursitis of the  
23 right knee on day 4 after tracer injection (days 0 and 2 not scanned; knees were not in the field  
24 of view on day 7; PET scans were performed once per patient and time point).



25

26 **Supplementary Figure 5**  $^{89}\text{Zr}$ -atezolizumab tumor uptake. (a) Relation between time post  
 27 tracer injection and tumor SUVmax ( $n = 196$  in 22 patients) plotted as geometric mean per  
 28 time point, including fitted regression line with 95%CI. (b) Relation between time post tracer  
 29 injection and tumor SUVmax for bladder cancer (yellow,  $n = 85$  in 9 patients) and NSCLC  
 30 (blue,  $n = 43$  in 9 patients) separately plotted as geometric mean per time point, including  
 31 fitted regression line with 95%CI. For TNBC (red,  $n = 68$  in four patients) no time-activity  
 32 curve was included as all four patients were only scanned at two time points, prohibiting  
 33 curve-estimation. (c) Relation between time post tracer injection and tumor-to-background  
 34 ratio of lung metastases (blue,  $n = 44$  in 10 patients) and bone metastases (orange,  $n = 62$  in 9

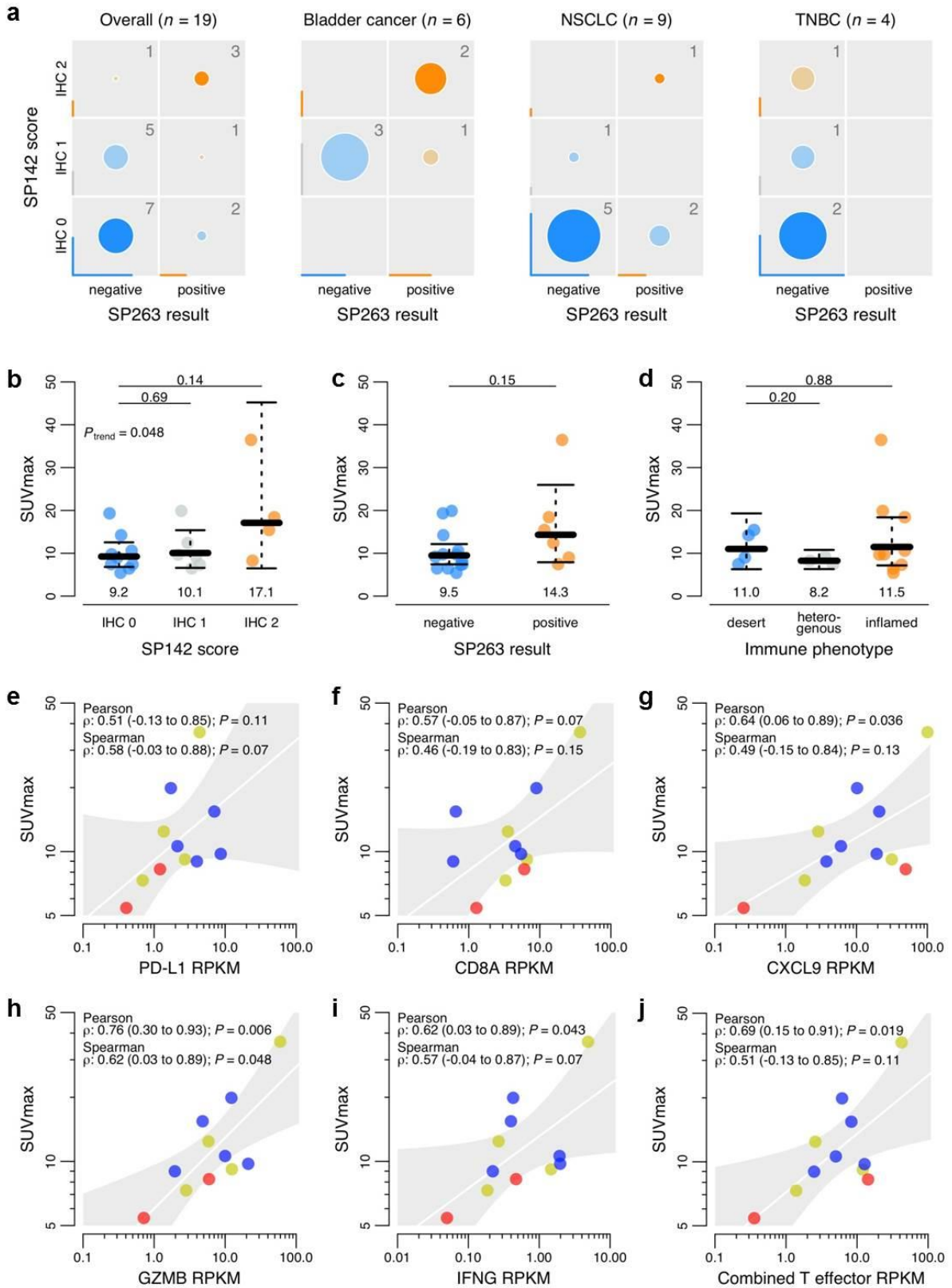
35 patients), as well as tumor-to-blood ratio (red,  $n = 196$  in 22 patients) plotted as geometric  
36 mean per time point, including fitted regression line with 95%CI. **(d)** Scatter plot of SUVmax  
37 day 4 and SUVmax day 7 and regression line with 95%CI based on a linear mixed effect  
38 model with 196 measurements from 22 patients;  $\rho$ : Pearson's correlation coefficient extended  
39 to clustered data with 95%CI.



40

41 **Supplementary Figure 6** Internalization of  $^{89}\text{Zr}$ -atezolizumab over time. (a) Internalization  
 42 of  $^{89}\text{Zr}$ -atezolizumab in vitro by H292 and H358 tumor cells ( $n = 3$  replicate wells). (b)  
 43 Internalization of  $^{89}\text{Zr}$ -atezolizumab in vitro by human peripheral blood mononuclear cells  
 44 (PBMCs) and T cells of healthy volunteers ( $n = 2$  replicate wells).

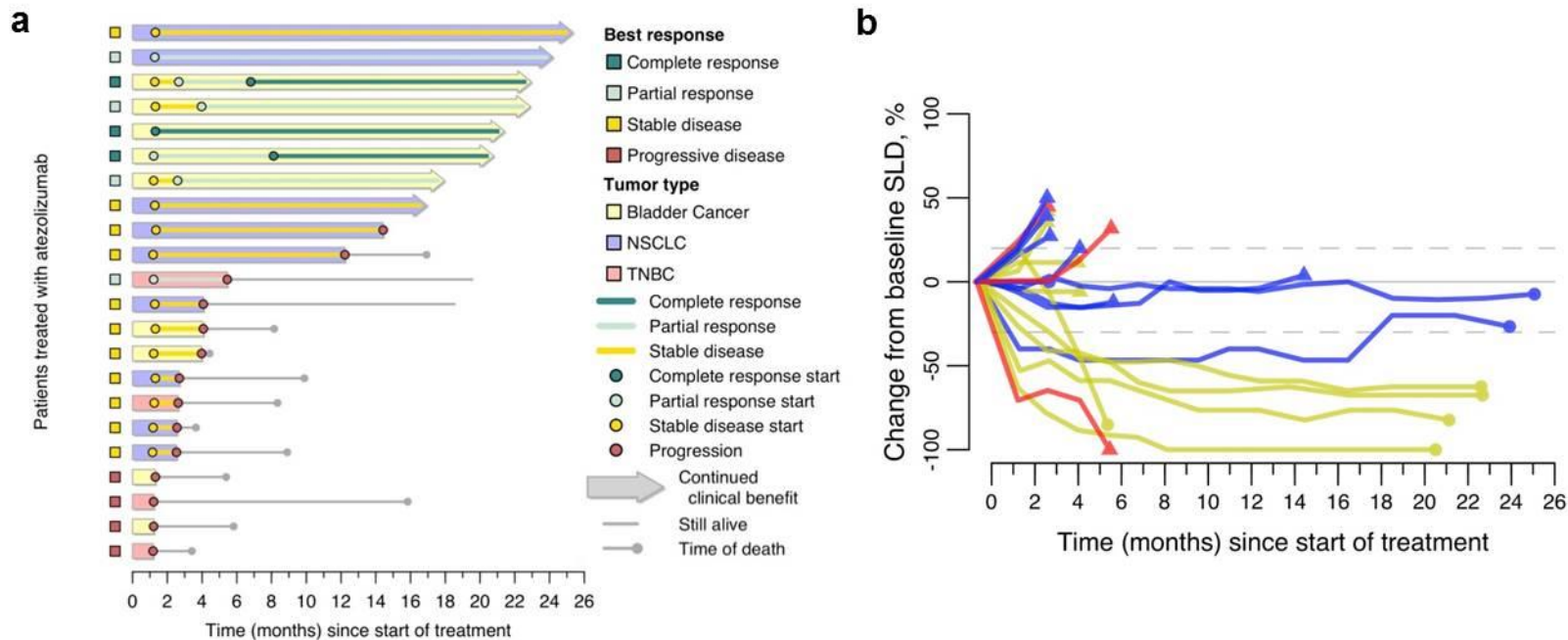




45

46 **Supplementary Figure 7** Relation of IHC, immune phenotypes, PD-L1 and T effector gene  
 47 expression levels with  $^{89}\text{Zr}$ -atezolizumab tumor uptake. (a) Confusion matrix of the  
 48 agreement in IHC results between the two tested PD-L1 antibodies, overall and according to

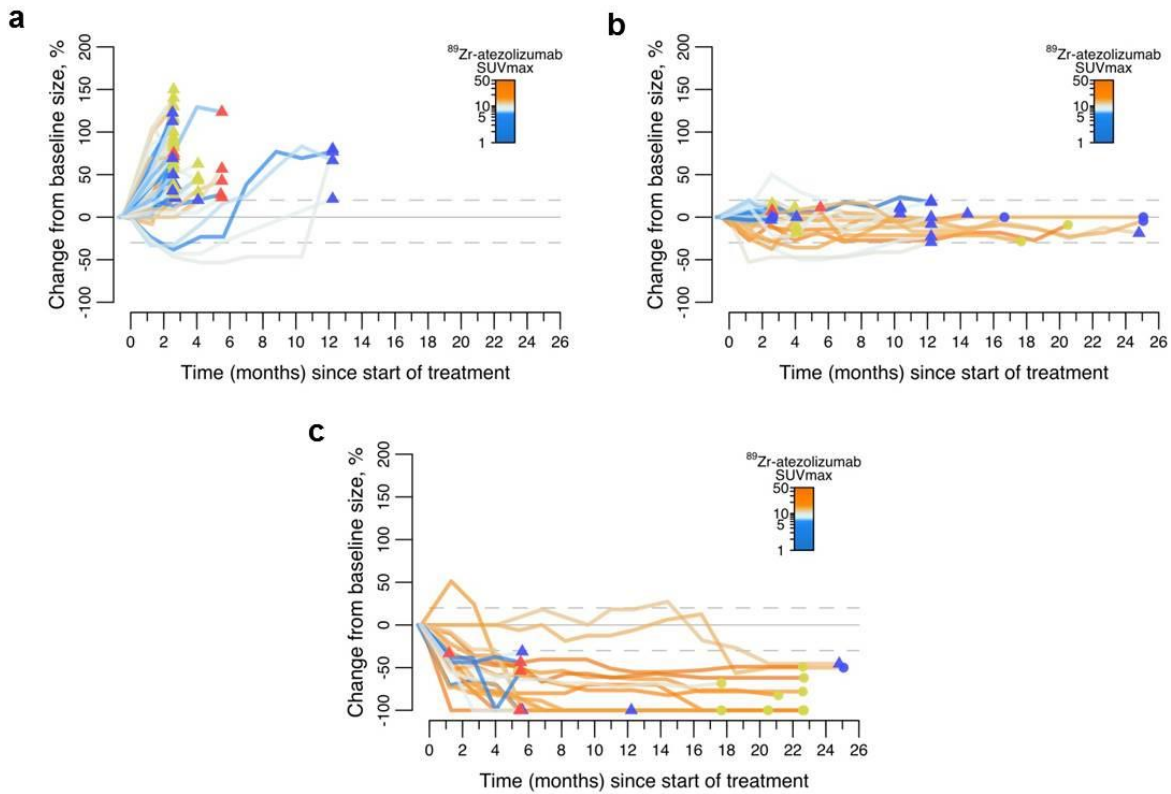
49 cancer type (size of circles corresponds with the relative distribution in each panel; marginal  
50 horizontal and vertical lines show the distribution per antibody). **(b-c)** Relationship between  
51 PD-L1 IHC (**(b)** SP142, **(c)** SP263;  $n = 19$  biologically independent samples) or **(d)** immune  
52 phenotype based on IHC ( $n = 16$  biologically independent samples) of biopsied lesions and  
53  $^{89}\text{Zr}$ -atezolizumab uptake on day 7 postinjection of the respective lesion. Data is summarized  
54 as geometric mean SUVmax with 95%CI as error bars; two-sided  $P$  values shown on top are  
55 derived from independent-samples t-tests, and the  $p$  for trend by linear regression. **(e-j)**  
56 Pearson's and Spearman's rank correlation (95%CI) of PD-L1 **(e)** and gene expression levels  
57 of CD8 **(f)**, chemokine ligand 9 **(g)**, granzyme B **(h)**, interferon gamma **(i)** and combined T  
58 effector signature **(j)** with  $^{89}\text{Zr}$ -atezolizumab uptake of the biopsied lesion ( $n = 11$  biologically  
59 independent samples); RPKM, reads per kilobase per million; red, TNBC; blue, NSCLC;  
60 yellow, bladder cancer.



61

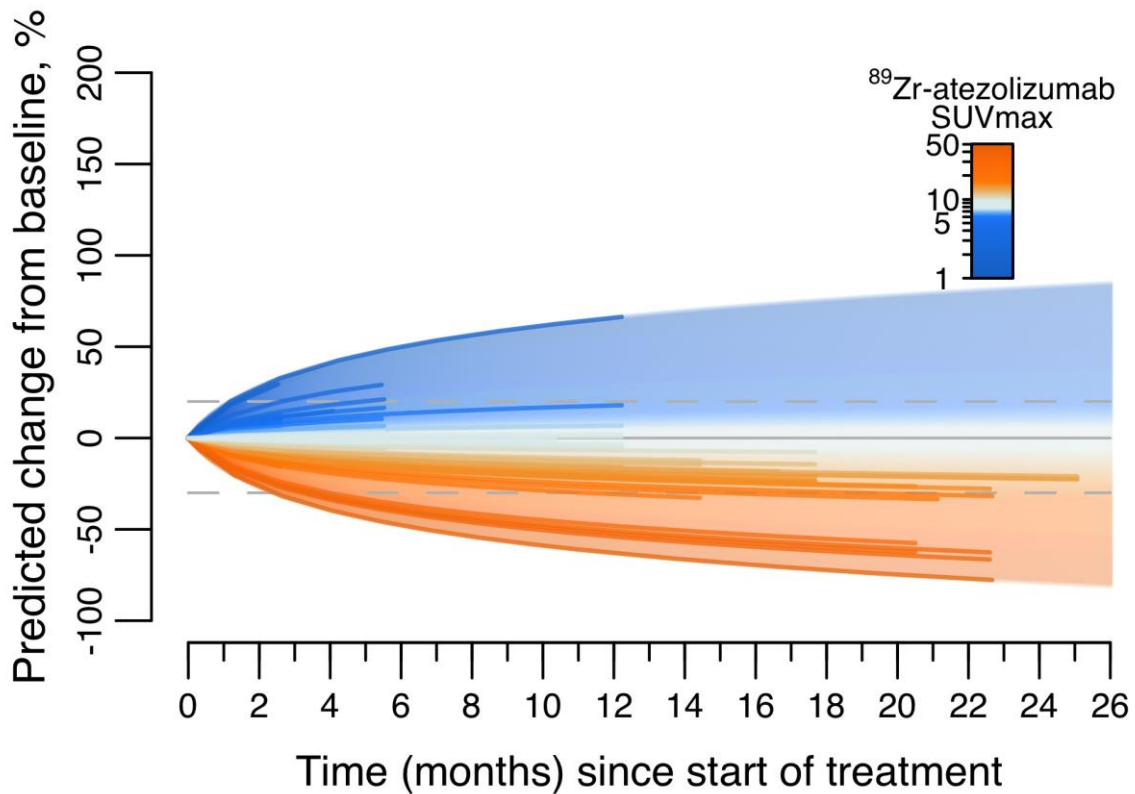
62 **Supplementary Figure 8** Response to atezolizumab monotherapy. **(a)** Swimmers plot of the 22 evaluable patients. **(b)** Change in baseline sum  
 63 of diameters (SLD; longest for non-nodal lesions, short axis for nodal lesions) per patient over time with dashed gray reference lines at +20%  
 64 and -30% change from baseline SLD. The circle or triangle at the end of the line represents ongoing tumor response or progressive disease,  
 65 respectively, at the last available moment of information regarding SLD (not necessarily corresponding with actual PD date). Line color  
 66 represents the tumor type (red, TNBC; blue, NSCLC; yellow, bladder cancer). At the data cut-off date of June 1 2018 seven patients were still

67 in follow-up: four of them were still on treatment, two were discontinued from treatment after 2 years and have an ongoing response, and one  
68 patient discontinued treatment despite clinical benefit due to side effects.



69

70 **Supplementary Figure 9** Spaghetti plots at lesion level grouped for tumor response per  
 71 lesion. Change in baseline diameter of single lesions (measured on CT; longest for non-nodal  
 72 lesions, short axis for nodal lesions; diameter > 20 mm) over time ( $n = 651$  measurements  
 73 from 107 metastases in 21 patients). Lines are color coded based on  $^{89}\text{Zr}$ -atezolizumab uptake  
 74 (SUVmax). The circle or triangle at the end of the line represents ongoing tumor response or  
 75 progressive disease, respectively, at the last available moment of patient based information  
 76 regarding SLD, and the color represents the tumor type (red, TNBC; blue, NSCLC; yellow,  
 77 bladder cancer). Lesions are grouped based on percent change in diameter from baseline  
 78 compared to last measurement ((**a**)  $\geq 20\%$ ; (**b**)  $> -30\%$  and  $< 20\%$ ; (**c**)  $\leq -30\%$ ) with dashed gray  
 79 reference lines at +20% and -30% change from baseline diameter.



80

81 **Supplementary Figure 10** Individual lesion's response to treatment. Graphical results of a  
 82 linear mixed effect model showing the relation of percent change from baseline size over time  
 83 and baseline SUVmax ( $n = 651$  measurements from 107 tumor lesions in 21 patients). The  
 84 colored lines are predicted trajectories of actual lesions measured in the study for the duration  
 85 of their actual observation, and the gradient filled area is a continuous representation of the  
 86 model.

87 **Supplementary Table 1. Demographics and disease characteristics of evaluable patients**  
 88 **(*n* = 22) at study entry.**

	All <i>n</i> = 22	Geometric mean SUV <sub>max</sub> <b>below</b> median <i>n</i> = 11	Geometric mean SUV <sub>max</sub> <b>above</b> median <i>n</i> = 11
Median age, years (range)	62.5 (40-76)	60 (42-71)	63 (40-76)
Sex, <i>n</i> (%)			
Male	13 (59)	5 (45)	8 (73)
Female	9 (41)	6 (55)	3 (27)
Primary tumor, <i>n</i> (%)			
BC	9 (41)	3 (27)	6 (55)
TNBC	4 (18)	4 (36)	0 (0)
NSCLC	9 (41)	4 (36)	5 (46)
ECOG performance status, <i>n</i> (%)			
0	14 (64)	7 (64)	7 (64)
1	8 (36)	4 (36)	4 (36)
Number of metastases, <i>n</i>			
Median (min-max)	4 (1-50)	5 (2-50)	3 (1-24)
Mean (SD)	8.9 (11.9)	12.2 (15.1)	5.6 (6.7)
Number of previous systemic regimens in the locally advanced or metastatic setting, <i>n</i> (%)			
1	15 (68)		
2	6 (27)		
≥3	1 (5)		

89 BC, Bladder cancer. TNBC, Triple-negative breast cancer. NSCLC, Non-small cell lung cancer. ECOG, Eastern  
 90 Cooperative Oncology Group. SUV, Standard uptake value.

91 **Supplementary Table 2. <sup>89</sup>Zr-atezolizumab and atezolizumab treatment-related adverse**  
 92 **events in 22 evaluable patients.**

		No. (%) of events	
		Any grade	Grade 3**
Tracer*	Pruritus	1 (100)	-
Atezolizumab	Alanine aminotransferase increased	2 (2)	-
	Alkaline phosphatase increased	1 (1)	-
	Alopecia	1 (1)	-
	Aspartate aminotransferase increased	3 (3)	-
	Anorexia	1 (1)	-
	Arthralgia	3 (3)	-
	Chills	1 (1)	-
	Diarrhea	3 (3)	-
	Dizziness	1 (1)	-
	Dry eyes	1 (1)	-
	Dry mouth	1 (1)	-
	Dry skin	4 (5)	-
	Edema	3 (3)	-
	QT corrected interval prolonged	1 (1)	-
	Fatigue	4 (5)	-
	Flatulence	1 (1)	-
	Flu like symptoms	2 (2)	-
	Hyperthyroidism	4 (5)	-
	Hypothyroidism	2 (2)	-
	Gammaglutamyltransferase increased	9 (10)	-
	Infusion related reaction	4 (5)	1 (1)
	Insomnia	2 (2)	-
	Myalgia	4 (5)	-
	Nausea	1 (1)	-
	Pain in extremity	7 (8)	-
	Paresthesia	2 (2)	-
	Platelet count decreased	1 (1)	-
Pneumonitis	1 (1)	-	
Pruritus	9 (10)	-	
Rash	7 (8)	-	

93 AE, Adverse event. \*Tracer comprises <sup>89</sup>Zr-labeled and unlabeled atezolizumab. \*\* No grade 4 events were  
 94 observed. No, number.



95 **Supplementary Table 3. Response rate per tumor type.**

Tumor type ( <i>n</i> )	CR ( <i>n</i> )	PR ( <i>n</i> )	SD ( <i>n</i> )	PD ( <i>n</i> )	ORR (%)
BC (9)	3	2	2	2	56
NSCLC (9)	0	1	8	0	11
TNBC (4)	0	1	1	2	25

96 BC, Bladder cancer. NSCLC, Non-small cell lung cancer. TNBC, Triple-negative breast  
 97 cancer. CR, Complete response. PR, Partial response. SD, Stable disease. PD, Progressive  
 98 disease. ORR, Objective response rate.

99 **Supplementary Table 4. Adjustment for tumor type and tumor load.**

100 1. Results of linear mixed-models with random intercept per patient relating best RECIST response to SUVmax  
 101 with various levels of adjustment ( $n = 22$  patients with 196 lesions):

Best RECIST response	Unadjusted			Adjusted for tumor type		
	% Difference in SUVmax	95%CI	<i>P</i>	% Difference in SUVmax	95%CI	<i>P</i>
PD	Reference	-	-	Reference	-	-
SD	41	-4 to 106	0.073	15	-26 to 79	0.49
PR	78	11 to 186	0.020	61	3 to 150	0.038
CR	235	98 to 467	0.00021	175	64 to 364	0.0013
Per category increase	45	24 to 69	2.24e <sup>-05</sup>	37	18 to 60	4.68e <sup>-05</sup>

102

Best RECIST response	Adjusted for tumor type and number of lesions			Adjusted for tumor type, number of lesions, lesion localization, VOI size		
	% Difference in SUVmax	95%CI	<i>P</i>	% Difference in SUVmax	95%CI	<i>P</i>
PD	Reference	-	-	Reference	-	-
SD	10	-33 to 81	0.68	3	-35 to 61	0.91
PR	53	-9 to 157	0.10	44	-10 to 130	0.12
CR	169	54 to 369	0.0025	110	26 to 249	0.0077
Per category increase	38	16 to 63	7.08e <sup>-05</sup>	28	10 to 50	0.00031

103

104 2. Results of relation between doubling in SUVmax and best percent change in SLD with various levels of  
 105 adjustment by linear regression ( $n = 21$  patients):

Model	Estimate	95%CI	<i>P</i>
Unadjusted	-34	-61 to 9	0.010
Adjusted for tumor type	-41	-68 to -13	0.0060
Adjusted for tumor type and number of lesions	-41	-70 to -11	0.0096

106

107 3. Relation between SUVmax and PFS/OS (HR for above median SUVmax per patient and below median  
 108 SUVmax) with various levels of adjustment:

Small sample bias corrected Cox (Firth)						
	Unadjusted			Adjusted for tumor type and load		
	HR	95%CI	<i>P</i>	HR	95%CI	<i>P</i>
All patients ( $n = 22$ )						
PFS	11.7	3.3 to 62.7	6.59e <sup>-09</sup>	10.0	2.2 to 62.4	0.0025
OS	6.3	1.8 to 33.4	0.0035	9.3	1.7 to 69.9	0.0084
Without TNBC ( $n = 18$ )						
PFS	10.7	2.7 to 59.6	0.00055	12.6	2.7 to 79.7	0.00097
OS	7.5	1.9 to 41.7	0.0041	12.4	2.3 to 99.2	0.0029

109

Regular Cox						
	Unadjusted			Adjusted for tumor type and load (IPW)*		
	HR	95%CI	<i>P</i>	HR	95%CI	<i>P</i>
All patients ( $n = 22$ )						
PFS	14.2	4.5 to 45.7	<0.001	14.7	4.4 to 45.7	<0.001
OS	8.4	2.4 to 30.0	0.0015	8.5	1.9 to 33.5	0.0008
Without TNBC ( $n = 18$ )						
PFS	13.2	4.1 to 40.9	<0.001	13.9	3.9 to 41.3	<0.001
OS	9.0	2.4 to 29.9	0.0030	9.2	1.6 to 33.5	0.020

110 \* Achieved balance assessed by post-IPW C-index (best 0.5; worst 1.0): All patients, tumor type and load  
 111 adjustment: 0.60; No TNBC, tumor type and load adjustment: 0.50.

112 **Supplementary Table 5. Continuous analysis of relationship between <sup>89</sup>Zr-atezolizumab**  
 113 **uptake and patient outcome.**

114

	<sup>89</sup> Zr-atezolizumab uptake as geometric mean SUVmax	
	PFS	OS
HR*	6.6	4.0
95%CI	2.3-26.7	1.5-16.1
<i>P</i> **	0.000032	0.0018

115 PFS, progression free survival; OS, overall survival; HR, hazard ratio. \* HR  
 116 per standard deviation decrease in the per patient geometric mean SUVmax. \*\*  
 117 Likelihood ratio *P*.

118 **Supplementary Table 6. Discriminatory performance of <sup>89</sup>Zr-**  
 119 **atezolizumab tumor uptake and PD-L1 IHC.**

	geometric mean <sup>89</sup> Zr- atezolizumab uptake (n = 22)	IHC SP142 (n = 19)	IHC SP263 (n = 19)
AUC (95%CI)*	0.83 (0.55-1.00)	0.60 (0.35-0.85)	0.63 (0.39-0.88)
C-index PFS (95%CI)	0.86 (0.69-1.00)	0.55 (0.39-0.70)	0.60 (0.45-0.76)
C-index OS (95%CI)	0.80 (0.61-1.00)	0.55 (0.37-0.73)	0.65 (0.47-0.82)

120 AUC, area under the receiver operating characteristics curve; IHC, immunohistochemistry; PFS, progression  
 121 free survival; OS, overall survival. \*Outcome defined as patients with and without CR/PR as best tumor  
 122 response.